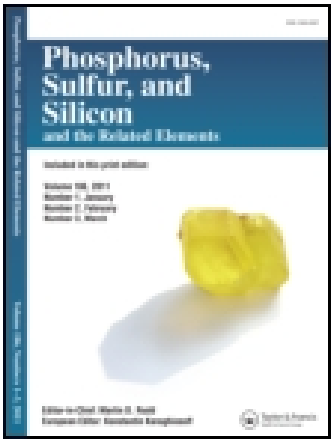

Phosphorus, Sulfur, and Silicon and the Related Elements
Publication details, including instructions for authors and subscription information:
http://www.tandfonline.com/loi/gpss20

Carbofunctional Silatrane Possessing Imidazole Moiety: Synthesis, Characterization, and Antibacterial Studies

Gurjaspreet Singh[a], Sheenam Girdhar[a], Raj Pal Sharma[a], Przemysław Starynowicz[b] & Baljinder Singh[c]

[a] Department of Chemistry, Panjab University, Chandigarh 160014, India

[b] Faculty of Chemistry, University of Wroclaw, Poland

[c] Department of Biotechnology, Panjab University, Chandigarh 160014, India

Accepted author version posted online: 26 Jun 2014.Published online: 16 Oct 2014.

To cite this article: Gurjaspreet Singh, Sheenam Girdhar, Raj Pal Sharma, Przemysław Starynowicz & Baljinder Singh (2014) Carbofunctional Silatrane Possessing Imidazole Moiety: Synthesis, Characterization, and Antibacterial Studies, Phosphorus, Sulfur, and Silicon and the Related Elements, 189:11, 1732-1745, DOI: 10.1080/10426507.2014.902822

To link to this article: http://dx.doi.org/10.1080/10426507.2014.902822

Phosphorus, Sulfur, and Silicon, 189:1732–1745, 2014

ISSN: 1042-6507 print / 1563-5325 online
DOI: 10.1080/10426507.2014.902822

CARBOFUNCTIONAL SILATRANE POSSESSING IMIDAZOLE MOIETY: SYNTHESIS, CHARACTERIZATION, AND ANTIBACTERIAL STUDIES

Gurjaspreet Singh,[1] Sheenam Girdhar,[1] Raj Pal Sharma,[1] Przemysław Starynowicz,[2] and Baljinder Singh[3]

[1]*Department of Chemistry, Panjab University, Chandigarh 160014, India*
[2]*Faculty of Chemistry, University of Wroclaw, Poland*
[3]*Department of Biotechnology, Panjab University, Chandigarh 160014, India*

GRAPHICAL ABSTRACT

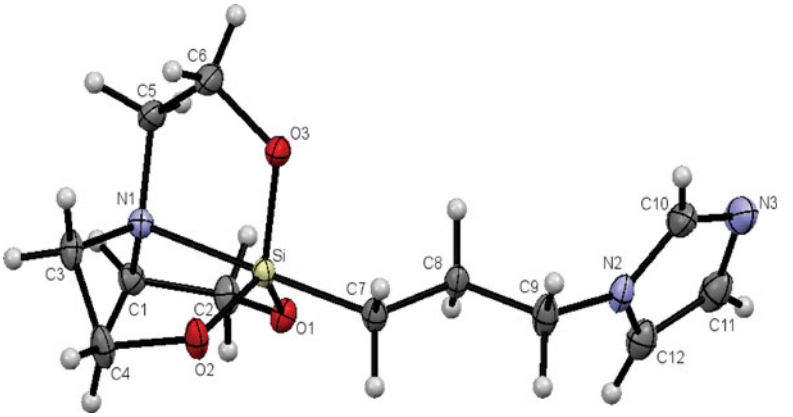

Abstract *1-(3-(1-imidazol-1-yl)propyl)-2,8,9-trioxa-5-aza-1-silabicyclo[3.3.3.0]undecane* ***3****, with imidazole functionality containing transannular N→Si bond (2.13 Å), was synthesized by transetherification reaction of triethanolamine* ***1*** *with N-(3-propyltriethoxysilane)imidazole* ***2****. The compound was characterized by elemental analysis, spectroscopic techniques (IR,* ^{1}*H NMR,* ^{13}*C NMR, UV–VIS), mass spectrometry, and X-ray diffraction. The thermal stability of silatrane* ***3*** *was studied by TGA/DTG/DSC techniques, which is in agreement with the mass spectrometry and X-ray diffraction studies. The structural investigations of* ***3*** *were complemented by quantum-chemical studies of the structure. Compound* ***3*** *showed slight activity against Escherichia coli and Staphylococcus aureus, while no activity was found against Bacillus subtillus and Vibrio cholera.*

Keywords Imidazole; silatrane; *N*-(3-propyltriethoxysilane)imidazole

Received 26 June 2013; accepted 26 January 2014.
Address correspondence to Dr. Gurjaspreet Singh, Assistant Professor, Department of Chemistry, Panjab University, Chandigarh 160014, India. E-mail: gjpsingh@pu.ac.in
Color versions of one or more of the figures in the article can be found online at www.tandfonline.com/gpss.

INTRODUCTION

Silatranes, cyclic organosilicon ethers of tris(2-oxyalkyl)amines or their derivatives, have been an expanse of profound study since their discovery in the early sixties.[1] The immense interest among researchers in these compounds was induced by their unusual polyhedral structure, the presence of a hypervalent X—Si—N fragment, their specific physical properties, the often unique reactivity, and a broad spectrum of biological activity.[2–4] In the recent years, organopropyl silatranes have been under close scrutiny by various researchers owing to the peculiarities of their electronic and molecular structure and diverse applications.[5–7]

Nitrogen heterocycles in silatranes have a long history and remain a front-runner for bioactive applications.[8] The imidazole ring is ubiquitous in nature and plays a critical role in many structures within the human body, notably as histamine and histidine.[9] Synthetic imidazoles are present in many fungicides and antifungal, antiprotozoal, and antihypertensive medications.[10–12] The presence of a donor pyridine-like nitrogen atom within the ring, capable of selective binding cationic species also converts the imidazole derivatives into excellent metal ion sensors.[13] The polar imidazole ring suggests a plethora of emerging material science and biophysical applications.[14] The silatranes containing imidazole moiety are scarce[15–16] and the motivation of this research stems from our previous work on silatranes.[17].

We report herein the preparation of 1-(3-(1-imidazol-1-yl)propyl)-2,8,9-trioxa-5-aza-1-silabicyclo[3.3.3] undecane **3** derived from triethanolamine **1** and *N*-(3-propyltriethoxysilane)-imidazole **2** as well as its structural characterization by single crystal X-ray diffraction, IR, ^{1}H NMR, ^{13}C NMR, UV–VIS and mass spectrometry. The thermal stability of **3** was studied using TGA/DTG/DSC techniques. Theoretical methods such as DFT and HF theory are very important for computing a molecular structure. So, the results obtained from X-ray crystallography were compared with theoretical studies such as DFT and HF methods. Anti-microbial activities of silatrane **3** were evaluated against bacterial culture of *Escherichia coli* and *Bacillus subtillus, Staphylococcus aureus* and *Vibrio cholera.*

RESULTS AND DISCUSSION

Synthesis

The triethoxysilane **2** was synthesized according to a method published earlier[18–19] (Scheme 1). The method of preparation was found to be propitious because of high yield of desired product as well as of its purity. Silatrane **3** was synthesized by transetherification reaction of **2** with **1** in the presence of KOH. The general reaction scheme for the synthesis of **3** is given below (Scheme 2). The product was stable in air and highly soluble in common organic solvents.

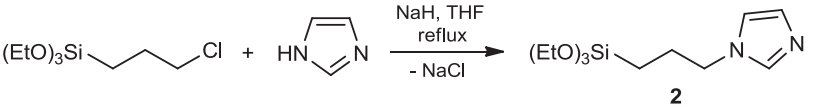

Scheme 1 Formation of triethoxysilane **2**.

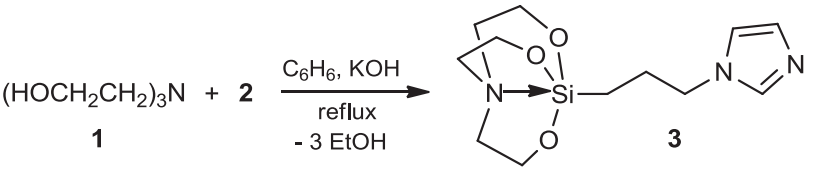

Scheme 2 Formation of silatranes **3**

Spectroscopic Studies

IR Spectroscopy. The IR spectra of compounds **2** and **3** were recorded in the range 4000–400 cm^{-1}. All bands observed for the silatranyl moiety were consistent with previous literature reports.[20,21] The absorption peaks of interest were those of Si—O, N→Si and C=N bonds. The bands at 1070 cm^{-1} and 1097 cm^{-1} were assigned to the ν(Si-O) stretching vibration in **2** and **3**, respectively. In addition, symmetric deformational vibration of the silatranyl skeleton with a predominant contribution from the bond N→Si was observed at 577 cm^{-1}. The bands observed at 1507 cm^{-1} and 1506 cm^{-1} for **2** and **3**, respectively, are the main characteristic bands indicating the presence of C=N group. Two bands observed at 1124 cm^{-1} and 940 cm^{-1} are characteristic for the symmetric and asymmetric stretching of the NC_3 fragment of the silatrane ring, respectively.

NMR Spectroscopy. The ^1H and ^{13}C NMR spectra are consistent with the structure of synthesized compound **3**. On comparing ^1H NMR spectra of **3** with those of **1**, a downfield shift for the OCH_2 and NCH_2 protons of $Si(OCH_2CH_2)_3N$ moiety in **3** was observed. All protons in the compound **3** were identified and the total number of protons calculated from the integration curve was found to be equal to expected number. In the ^1H NMR spectrum of compound **3** an upfield shift was observed for $SiCH_2$ protons as compared to **2**, which clearly indicates an increase in electron density at silicon due to the formation of N→Si dative bond. A triplet appears for the $SiCH_2$ protons at 0.30 ppm due to the presence of a direct Si–C bond. In addition, a multiplet due to the protons of the CCH_2C fragment at 1.17 ppm was also observed. In the ^{13}C NMR spectrum of silatrane **3** the most shielded carbon atom belongs to the Si-CH_2 moiety and is observed at 13.2 ppm. The signals observed at 119.0, 128.8, and 137.1 ppm are assigned to the imidazole ring carbon atoms.

Mass Spectrometry. Mass spectra of compound **3** showed the molecular ion peaks with the addition of H and Na and their fragmentation displays the common features of silatranes.[22] The molecular ion peak, which is also the base peak, appears in the spectra as $[M+H]^+$ at $m/z = 284$. The molecular ion peak was more abundant as compared to silatranyl ion peak. The fragmentation pattern of **3** is shown in Scheme 3.

UV–VIS Spectra. The UV spectra of complex **3** when recorded in ethanol gave a peak at 250 nm which was attributed to the π–π^* transition[23,24] in the imidazole group with a molar extinction coefficient $\varepsilon = 2.7 \times 10^2$ M^{-1} cm^{-1} (Figure 1). This long wavelength π–π^* absorption band successfully experienced a redshift in silatrane **3** relative to that in the free imidazole[25] which showed that the introduction of silatranylpropyl group on the imidazole ring markedly perturbed the low energy π–π^* transition in UV spectra of imidazole similar to that of other azoles such as pyrrole, indole, and carbazole.[26].

Thermogravimetric Analysis. Thermogravimetric analysis (TGA) curve of compound **3** was recorded to study its thermal stability. The complex was heated from 25 to 1000°C under nitrogen atmosphere. The TGA curve of compound **3** shows mainly two steps: the first corresponds to the loss of imidazole moiety (calc. = 23.09%, expt. = 23.67%) in

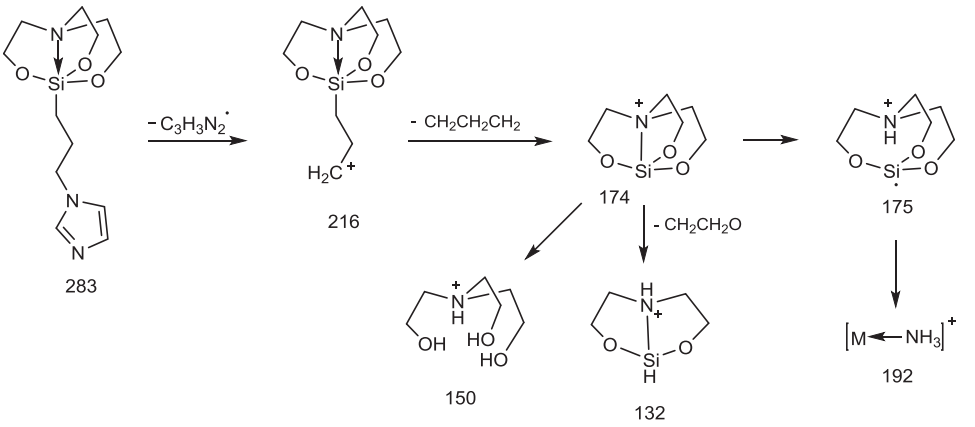

Scheme 3 Mass fragmentation pattern of compound **3**.

the temperature range 110–180°C, which was also confirmed by the mass spectrum of **3**; the second step shows the weight loss of the rest of the molecule (calc. = 76.91%, expt. = 76.33%) starting from 225°C (Figure 2). The maximum weight loss was indicated by the DTG peak at 265°C (Figure 3). In DSC, a small endothermal peak was observed at about 118°C, which was assigned to its melting point (Figure 4).

X-Ray Crystallography. Single crystal X-ray diffraction study showed that compound **3** crystallized in a monoclinic crystal system. The X-ray data, selected bond distances, and angles of compound **3** are listed in Table 1 and 2. An ORTEP type view of **3** with atomic labeling is shown in Figure 5 (thermal ellipsoids have been drawn at 50% probability level). The five atoms bonded to the silicon atom form a distorted trigonal bipyramid; such geometry is imposed by the coordination of the tripodal triethanolamine

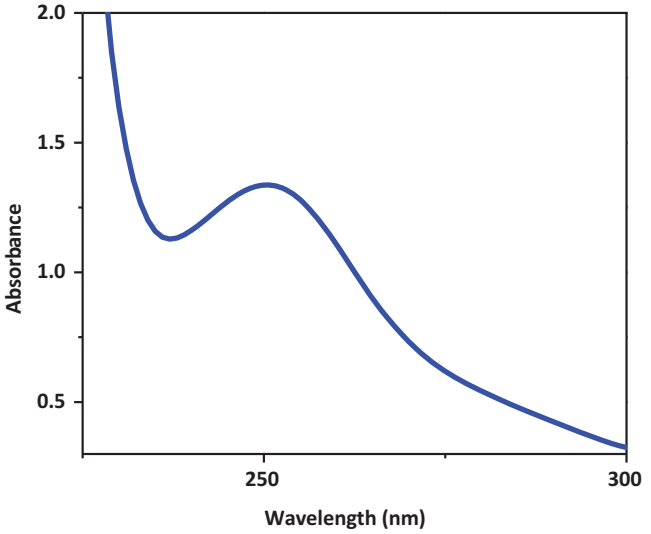

Figure 1 UV–VIS spectrum of **3** (5 mM solution in ethanol).

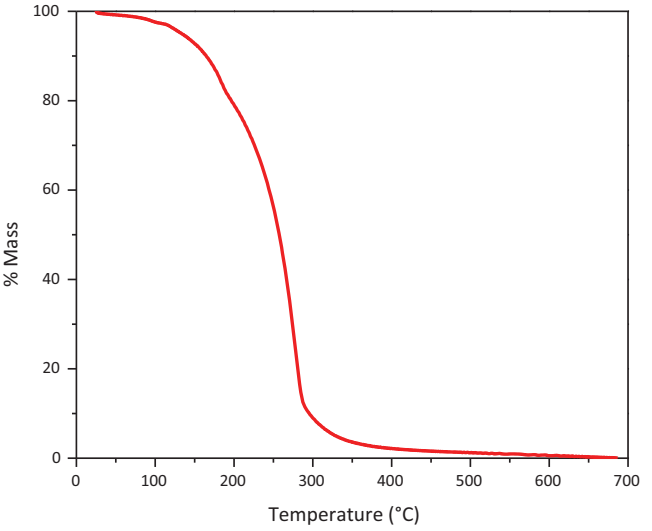

Figure 2 TGA curve of compound **3**.

fragment. The O atoms of the tetradentate ligand occupy equatorial positions and the N donor is present at apical site *trans* to the imidazole functionalized alkyl chain. The most noteworthy parameter is the N→Si bond length of 2.138(2) Å. This value is close to the average distance in the $N(C_2H_4O)_3SiC$ fragments, 2.146(52) Å, calculated out of 126 fragments retrieved from the CCDC data base. The minimum reported value of this distance, 1.965(5) Å, was found in 1-(dimethyloxonio)silatranium tetrafluoroborate, $[(CH_3)_2O^+$-$Si(OCH_2CH_2)_3N]BF_4$.[27] The shortest N→Si bond (2.095 Å) in a silatrane with a Si–C bond was found in 1-[(silatranyl)methyl]-1,2,4-triazole.[28] On the other hand, the longest

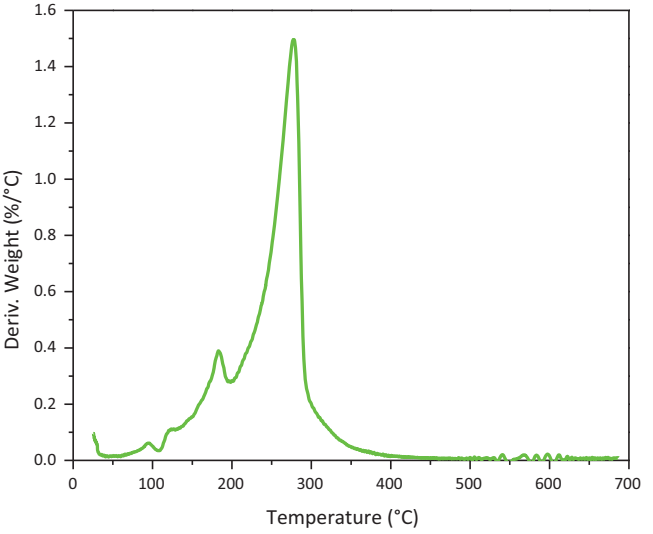

Figure 3 Deriv. TGA curve of compound **3**.

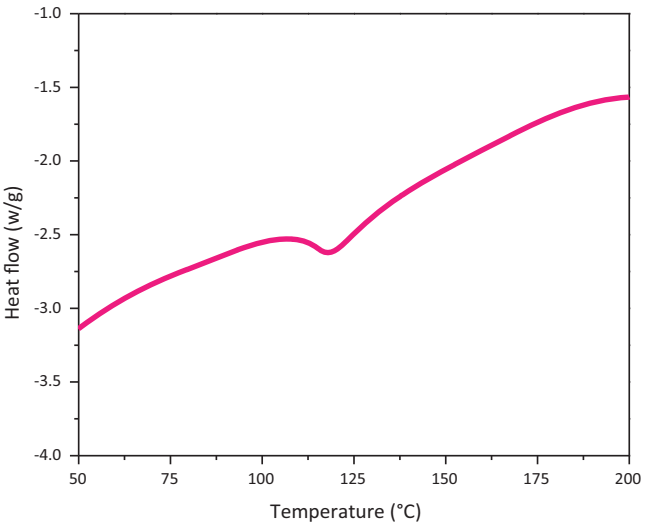

Figure 4 DSC curve of compound **3**.

N→Si bonds, 2.421 and 2.32 Å, for this subgroup of silatranes, were observed in 8-dimethylamino-1-naphthyl)silatrane[29] and (-)-(4R,6R,11R)-1,4,6,11-tetramethylsilatrane, $ClC_3H_6Si(OCH_2CH_2)_2$ $[OCH_2CH(COOH)]N{\cdot}H_2O$[30], respectively.

The present N→Si bond distance is noticeably shorter than the sum of the van der Waals radii (3.5 Å) and indicates a weak bonding interaction between both the atoms. The N—Si—C is a three center four-electron hypervalent bond. The bond angles around

Table 1 Details on X-ray data collection and structure refinement of compound **3**

Chemical formula	$C_{12}H_{21}N_3O_3Si$
M_r	283.41
Crystal system, space group	Monoclinic, $P2_1/n$
Temperature (K)	100
a, b, c (Å)	6.569(2), 11.756(4), 18.287(6)
β (°)	95.62(3)
V (Å^3)	1405.4(8)
Z	4
Radiation type	Mo $K\alpha$
μ (mm^{-1})	0.18
Crystal size (mm)	0.43 × 0.33 × 0.18
Data collection	
T_{min}, T_{max}	0.949, 0.976
No. of measured, independent, and observed [$I > 2\sigma(I)$] reflections	9784, 3410, 2718
R_{int}	0.032
Refinement	
$R[F^2 > 2\sigma(F^2)]$, $wR(F^2)$, S	0.045, 0.124, 1.10
No. of reflections	3410
No. of parameters	172
No. of restraints	0
H-atom treatment	H-atom parameters constrained
$\Delta\rho_{max}$, $\Delta\rho_{min}$ (e Å^{-3})	0.48, −0.28

Table 2 Selected bond lengths (Å) and angles (°) of silatrane **3**

Si—O2	1.6695 (13)	N2—C10	1.342 (2)
Si—O1	1.6696(13)	N2—C12	1.368(2)
Si—O3	1.6737(12)	N2—C9	1.468(2)
Si—C7	1.8887(17)	C1—C2	1.519(2)
Si—N1	2.1379(14)	C3—C4	1.517(2)
O1—C2	1.4184(19)	C5—C6	1.517(2)
O2—C4	1.4299(19)	C7—C8	1.536(2)
O3—C6	1.426(2)	C8—C9	1.515(2)
N1—C5	1.473(2)	C10—N3	1.322(2)
N1—C1	1.473(2)	N3—C11	1.373(3)
N1—C3	1.477(2)	C11—C12	1.371(3)
O2—Si—O1	118.30(7)	C3—N1—Si	104.48(9)
O2—Si—O3	118.53(7)	C10—N2—C12	106.68(15)
O1—Si—O3	119.37(6)	C10—N2—C9	126.82(16)
O2—Si—C7	97.82(7)	C12—N2—C9	126.41(16)
O1—Si—C7	95.39(7)	N1—C1—C2	105.68(12)
O3—Si—C7	96.33(7)	O1—C2—C1	109.04(13)
O2—Si—N1	84.01(6)	N1—C3—C4	105.57(12)
O1—Si—N1	83.02(6)	O2—C4—C3	108.05(13)
O3—Si—N1	83.44(6)	N1—C5—C6	105.97(13)
C7—Si—N1	178.00(6)	O3—C6—C5	108.42(13)
C2—O1—Si	123.16(10)	C8—C7—Si	113.96(11)
C4—O2—Si	121.32(10)	C9—C8—C7	113.40(13)
C6—O3—Si	122.40(10)	N2—C9—C8	112.24(13)
C5—N1—C1	112.98(12)	N3—C10—N2	113.03(17)
C5—N1—C3	114.02(13)	C10—N3—C11	104.11(16)
C1—N1—C3	113.16(12)	C12—C11—N3	110.43(17)
C5—N1—Si	105.11(9)	N2—C12—C11	105.76(17)
C1—N1—Si	106.00(9)		

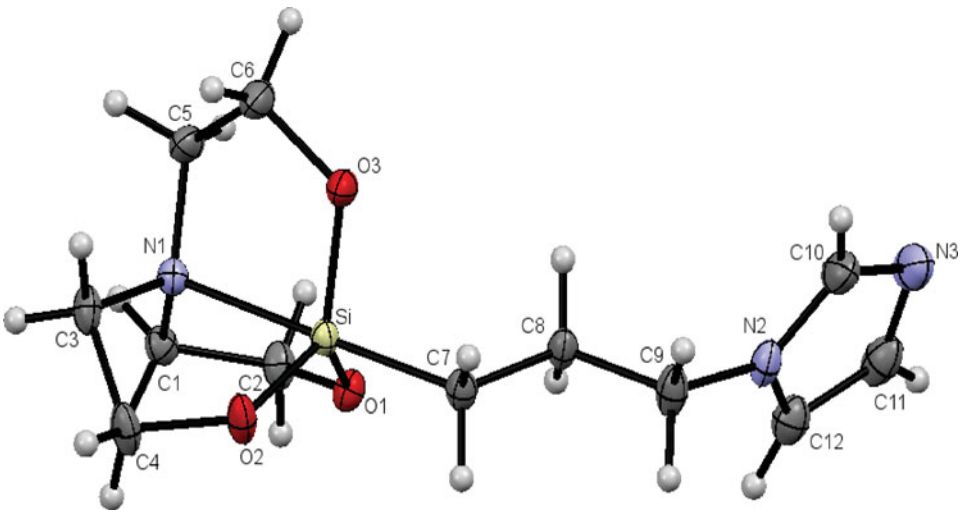

Figure 5 ORTEP diagram of compound **3**.

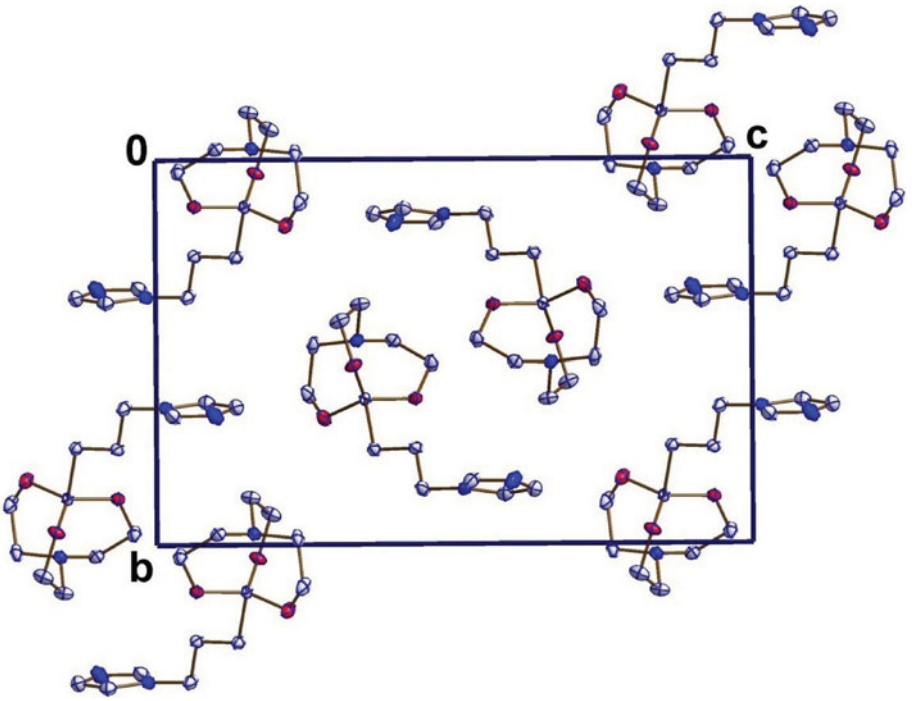

Figure 6 Packing diagram of compound **3**.

the silicon atom may be discussed in terms of pentacoordination character, i.e., percentage trigonal bipyramid (%TBP). The pentacoordination character could be calculated from three apical-to-equatorial bond angles and three equatorial-to-equatorial bond angles according to the Equations (1) and (2). % TBPax and % TBPeq for compound **3** were 66.56% and 88.95%.

$$\%\text{TBPax} = 100\%\,[\{109.5 - 1/3\Big(\sum{}^{\theta}\text{n}\Big)\}/(109.5 - 90.0)] \quad (1)$$

$$\%\text{TBPeq} = 100\%\,[\{1/3\Big(\sum{}^{\theta}\text{n}\Big) - 109.5\}/(120.0 - 109.5)] \quad (2)$$

where θ_n is average of angles $O_{eq}{-}Si{-}C_{ax}$ and φ_n is average of angles $O_{eq}{-}Si{-}O_{eq}$.

The values of the %TBP parameters show that the figure spanned by O1, O2, O3, and C7 may be described as a trigonal pyramid distorted toward a tetrahedron. The crystal is held together with van der Waals forces only. The shortest intermolecular contacts are: O1···C10 $(1 + x, y, z) - 3.246(3)$ Å (O1···H10 $(1 + x, y, z) - 2.62$ Å), O2···C5 $(\frac{1}{2}{-}x, \frac{1}{2} + y, \frac{1}{2} - z) - 3.417(3)$ Å (O1···H5A $(\frac{1}{2}{-}x, \frac{1}{2} + y, \frac{1}{2} - z) - 2.47$ Å), O3···C1 $(-1 + x, y, z) - 3.451(3)$ Å (O3···H1B $(-1 + x, y, z) - 2.55$ Å) and N3···C4 $(-3/2 - x, \frac{1}{2} - y, -\frac{1}{2} + z) - 3.435(3)$ Å (N3···H4A $(-3/2 - x, \frac{1}{2} - y, -\frac{1}{2} + z) - 2.56$ Å). The packing diagram is shown in Figure 6.

A comparative study of some characteristic geometrical features of previously reported γ-organopropyl silatranes 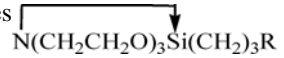 has been summarized in Table 3.

Table 3 Comparison of some characteristic geometrical data of γ-organopropyl silatranes $N(CH_2CH_2O)_3Si(CH_2)_3R$

R	N→Si (Å)	Si-$O_{av.}$ (Å)	NSiC (°)	$NSiO_{mean}$(°)	% TBP_{ax}	% TBP_{eq}	Lit.
$C_3H_3N_2$	2.13	1.67	178.00	83.49	66.56	88.95	This work
NCS	2.16	1.65	178.34	82.60	64.46	86.34	[31]
SH	2.17	1.65	178.60	82.70	62.66	84.76	[32]
OH	2.17	1.66	179.80	82.70	62.56	85.04	[33]
NH_2	2.17	1.66	179.10	82.74	62.76	84.95	[34]

Computational Studies. Density Functional Theory (DFT) and Hartree–Fock (HF) calculations were performed for compound **3** with the GAUSSIAN 03 software package[35,36] at the 6-31+G*(d) and 3-21+G* level of theory (Figure 7). The various geometrical parameters obtained from the crystal data were further compared with the calculated values obtained from the HF methods and DFT as shown in Table 4.

There were discrepancies between some parameters around the silicon atom for both gas and solid phases, i.e., crystal-phase structure. The bond angle around the silicon atom, such as N(1)–Si–C(7), was an important factor to judge how much the geometry around the silicon atom deviated from a pentacoordinated trigonal bipyramidal structure. In this theoretical study, however, the N(1)–Si–C(7) bond angle in the gas phase was found to be around 180° whereas the experimentally determined N(1)–Si–C(7) bond angle was 178.0°. The most significant geometrical parameter of the silatranes, the N→Si bond length, was found calculated to be relatively longer than that retrieved from the crystal data. This discrepancy may be due to a shallow vibrational potential of the N→Si bond[37–41] and influence of crystal packing forces. The X-ray studies demonstrated that the bond lengths Si—O av.,

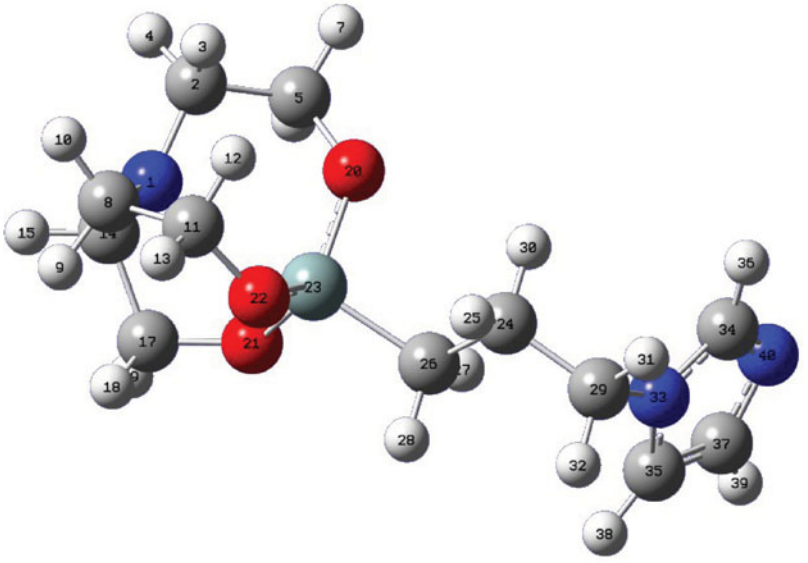

Figure 7 Optimized structure of compound **3**.

Table 4 Calculated and X-ray crystallographic data of compound **3**

PParameters	X-ray crystal data	DFT, B3LYP 3-21G*	DFT, B3LYP 6-31G*(d)	RHF, 3-21G*	RHF, 6-31G*(d)
N(1)→Si	2.13	2.31	2.60	2.31	2.70
Si-O av.	1.66	1.71	1.67	1.71	1.64
Si-C7	1.88	1.89	1.87	1.89	1.86
N(2)-C(9)	1.46	1.47	1.46	1.46	1.46
N(1)-C(1,3,4)	1.38	1.43	1.44	1.43	1.44
N(2)-C(10)	1.34	1.38	1.36	1.38	1.34
N(3)-C(10)	1.32	1.33	1.31	1.33	1.29
N(2)-C(10)-N(3)	113.03	111.78	112.45	111.78	112.88
C(9)-N(2)-C(10)	126.82	126.25	126.45	126.25	126.66
C(7)-C(8)-C(9)	*113.40*	*113.32*	114.38	113.32	114.27
C(8)-C(7)-Si	113.96	111.99	115.15	111.99	115.12
N(1)-Si-C(7)	178.00	179.76	179.32	179.76	179.46
O(1)-Si-O(2)	118.30	118.04	113.22	118.04	112.44
O(1)-Si-O(3)	119.37	117.70	114.50	116.76	114.68
O(2)-Si-O(3)	118.53	116.76	113.71	117.76	111.79
C(5)-N(1)-Si	105.11	103.60	98.66	103.45	96.65

Si–C, N(2)–C(9), N(2)–C(10) and the bond angles N(2)–C(10)–N(3), C(9)–N(2)–C(10), C(7)–C(8)–C(9) were in accordance with the theoretical data. The variation in other bond lengths and angles was attributed to the denser packing of molecules which promotes the intensification of intermolecular interactions and, hence, compression of the molecules.

Biological Activity. To investigate the antibacterial activity compound **3** was dissolved in DMSO and the sample was tested in triplicate. DMSO alone was taken as control and results were compared with control. Antibacterial activity is classified as highly active (>14 mm), moderately active (10–14 mm), slightly active (6–10 mm), and less than 5 mm is taken as inactive.[42]

The minimum inhibitory concentration (MIC) of compound **3** was determined using micro-broth dilution method. In the broth dilution MIC method, various concentrations of the compound are inoculated with a standard suspension of test bacteria. Following an overnight incubation at 35°C, the MIC is determined by observing the lowest concentration of the compounds that will inhibit visible growth of the test bacteria. Growth was determined photometrically by measuring the optical density (OD) at 600 nm.

$$\text{Percentage of growth} = \frac{\text{OD of organism grown with sample}}{\text{OD of control}}.$$

The inhibition zone diameter after 12 h was found to be 6 mm for *E. coli* and *Staphylococcus aureus*. MIC_{50} (defined as the minimum concentration at which 50% of the isolates were inhibited) of compound **3** against *E.coli* and *Staphylococcus aureus* was 120 ± 2 mg/mL.

EXPERIMENTAL

Syntheses

The syntheses were carried out under dry nitrogen atmosphere using vacuum glass line. The organic solvents used were dried and purified according to standard procedures.

3-Chloropropyltriethoxysilane (Aldrich) and triethanolamine (Merck) were used as received from supplier. *N*-(3-Propyltriethoxysilane)imidazole **2** was synthesized according to reported method.

Characterization

Infrared spectra were routinely obtained as Nujol mulls with a Perkin-Elmer RX-I FT IR spectrometer. C, H, and N analyses were obtained with a FLASH-2000 Organic Elemental Analyzer. Mass spectrometric measurements (TOF MS, ES^+, 1.38 eV) were carried out with a VG Analytical (70-S) spectrometer. The electronic spectrum in ethanol as a solvent was monitored using 10 mm quartz cells with Jasco UV–VIS spectrophotometer model V-530. The ^1H and ^{13}C NMR spectra were recorded with a Jeol and Bruker FT NMR (AL 300 MHz) spectrometer using $CDCl_3$ as solvent. Chemical shifts are reported in ppm relative to tetramethylsilane.

X-Ray Diffraction Studies

An appropriate crystal of **3** was cut from a larger one and mounted on a Kuma KM4 diffractometer equipped with a CCD counter. The collected data were corrected for polarization, Lorentz, and absorption, the last calculated from the crystal habits captured from photo scans. The structure was solved and refined routinely with SHELXS97 and SHELXL97 programs.[43,44] The positions of the hydrogen atoms (all of them are C-bonded) were calculated geometrically. All non-H atoms were refined anisotropically, the positions of the H atoms were geometrically constrained and their isotropic temperature factors were constrained as 1.2 of the trace of the thermal vibration tensors of the parent C atoms. The pertinent data are given in Table 1.

Thermogravimetric Analyses

TGA/DTG/DSC analyses were run on SDT Q 600V20.9 Build 20TGA Instrument. The sample was loaded in alumina pans and ramped at 10°C/min over a temperature range of 25–1000°C in dry air at 60 mL/min.

Theoretical Studies

The quantum mechanical calculations were performed with the Gaussian 03 series programs. Geometries were optimized using Hartree–Fock (HF) calculations and Density Functional Theory (DFT), using Becke's three parameter hybrid exchange functional and the correlation functional of Lee, Yang, and Parr (B3LYP) with basis set at 3-21G* and 6-31G*(d) level of theory.

Assessment of Antibacterial Activity

Disk Diffusion Method. Antimicrobial activity was determined by the disk diffusion method. In this technique, the filter paper (Whatsmann no. 1) sterile disc of 5 mm diameter impregnated with test compounds (20, 40, 60, 80, 100 mg/mL of DMSO) were placed in nutrient agar plate at 37°C for 12 h. The inhibition zones around the dried impregnated disks were measured after 12 h.

Test Microorganism. Test isolates were taken from the MTCC (Microbial Type Culture Collection) at the Institute of Microbial Technology (IMTECH), Chandigarh, India and included *Escherichia coli* and *Bacillus subtillus, Staphylococcus aureus and Vibrio cholera.*

Synthesis of *N*-(3-propyltriethoxysilane)imidazole 2. To a suspension of NaH (0.52 g, 22 mmol) in anhydrous THF (55 mL) at 0°C was added imidazole (1.5 g, 22 mmol) and the mixture was allowed to stir for 30 min. 3-Chloropropyltriethoxysilane (5.29 g, 22 mmol) was then added to the reaction mixture at 0°C. The reaction mixture was allowed to warm to room temperature and stirred under reflux for a further 24 h. The reaction mixture was cooled to room temperature, filtered and washed with ether. The filtrate was concentrated *in vacuo* and a colorless oil was separated as the final product, which was used as such without any further purification. ^{1}H NMR ($CDCl_3$): $\delta = 0.61$ (t, $J = 8.1$ Hz, 2H, $SiCH_2$), 1.12 (t, $J = 7.1$ Hz, 6H, CH_3), 1.76 (m, 2H, CCH_2C), 3.40 (t, $J = 7.8$ Hz, 2H, CCH_2N), 3.70 (q, $J = 7.1$ Hz, 9H, OCH_2), 6.82 (s, 1H, imidazole-H), 7.39 (s, 1H, imidazole-H), 7.68 (s, 1H, imidazole-H). ^{13}C NMR ($CDCl_3$): $\delta = 7.7$ ($SiCH_2$), 17.8 (CH_3), 26.1 ($C\boldsymbol{C}H_2C$), 46.6 ($C\boldsymbol{C}H_2N$), 57.7 (OCH_2), 118.2, 120.9, 134.4 (imidazole-C). IR (Nujol, cm^{-1}): 1070 (ν (as)Si—OC), 1507 (ν (as)C=N).

Synthesis of 1-(3-(1-Imidazol-1-yl)propyl)-2,8,9-trioxa-5-aza-1-silabicyclo[3.3.3] undecane (3). *N*-(3-Propyltriethoxysilane)imidazole (1.00 g, 3.68 mmol) was added to triethanolamine (0.55 g, 3.68 mmol) in anhydrous benzene with a catalytic amount of KOH at room temperature in a two-necked flask fitted with a Dean Stark trap. The resulting mixture was refluxed for 5 h to remove azeotropically the ethanol formed during the reaction. The solvent was evaporated under vacuum and 10 mL of ether was added. The content was stirred for 30 min and the product was isolated as a white powder. The solid was filtered and dried under vacuum. White needle-shaped crystals suitable for single crystal X-ray analyses were separated after 2 days from the ether extract. M.p.: 118°C, Yield: 0.87 g, 84%. Anal. Calcd. for $C_{15}H_{27}N_3O_3Si$: C, 55.35; H, 8.36; N, 12.91; Si, 8.63. Found: C, 55.32; H, 8.34; N, 12.88; Si, 8.64%. IR (Nujol, cm^{-1}): 1093 (ν(as)Si—OC), 622 (ν (as)N→Si), 1506 (ν(as)C=N). ^{1}H NMR ($CDCl_3$): $\delta = 0.30$ (m, 2H, $SiCH_2$), 1.76 (m, 2H, CCH_2C), 2.72 (t, $J = 5.8$ Hz, 6H, NCH_2), 3.67 (t, $J = 5.8$ Hz, 6H, OCH_2), 3.77 (t, $J = 7.8$ Hz 2H, CCH_2N), 6.84 (s, 1H, imidazole-H), 6.92 (s, 1H, imidazole-H), 7.39 (s, 1H, imidazole-H). ^{13}C NMR ($CDCl_3$): $\delta = 13.2$ ($SiCH_2$), 27.2 ($C\boldsymbol{C}H_2C$), 50.3 ($C\boldsymbol{C}H_2N$), 51.1 (NCH_2), 57.6 (OCH_2), 119.0, 128.8, 137.1 (imidazole-C). MS (m/e, relative intensity, assignment): 284 [100, M + H]$^+$, 216.1 [3.33, $CH_2CH_2CH_2Si(OCH_2CH_2)_3N$], 174.1 [27.48, $Si(OCH_2OCH_2)_3N^+$], 306 [8.06, M+Na]$^+$.

CONCLUSION

A synthetic methodology for the synthesis of silatrane 1-(3-(1-imidazol-1-yl)propyl)-2,8,9-trioxa-5-aza-1-silabicyclo[3.3.3]undecane has been outlined. The product obtained has been characterized by various physicochemical techniques and its structure confirmed by single crystal X-ray diffraction. In the present study, anti-microbial activities of silatrane **3** were evaluated against bacterial culture of *Escherichia coli* and *Bacillus subtillus, Staphylococcus aureus and Vibrio cholera.* The compound showed slight activity against *Escherichia coli* and *Staphylococcus aureus* but no activity was found against *Bacillus subtillus* and *Vibrio cholera.* The results obtained clearly indicated that the compound **3** was not active toward growth inhibition of Gram negative and Gram positive bacteria under this

investigation. Instead bacteria(s) utilized these compounds as a source of carbon, nitrogen and energy.

FUNDING

The authors are thankful to UGC, New Delhi (India) for providing financial support.

SUPPLEMENTAL MATERIAL

Supplementary data for this article can be accessed on the publisher's website, www.tandfonline.com/gpss

CCDC-927330 contains the supplementary crystallographic data for this paper. These data can be obtained free of charge from The Cambridge Crystallographic Data Centre via www.ccdc.cam.ac.uk/data_request/cif.

REFERENCES

1. Frye, C. L.; Vogel, G. E.; Hall, J. A. *J. Am. Chem. Soc.* **1961,** 83, 996-997.
2. Voronkov, M. G. *Top. Curr. Chem.* **1979,** 84, 77-135.
3. Verkade, J. G. *Coord. Chem. Rev.* **1994,** 137, 233-295.
4. Puri, J. K.; Singh, R.; Chahal, V. K. *Chem. Soc. Rev.* **2011,** 40, 1791-1840.
5. Singh, R.; Puri, J. K.; Sharma, R. P.; Malik, A. K.; Ferretti V. *J. Mol. Struct.* **2010,** 982, 107-112.
6. Puri, J. K.; Singh, R.; Chahal, V. K.; Sharma, R. P.; Wagler, J.; Kroke E. *J. Organomet. Chem.* **2011,** 696, 1341-1348.
7. Singh, R.; Mutneja, R.; Kaur, V.; Wagler, J.; Kroke, E. *J. Organomet. Chem.* **2013,** 724, 186-191.
8. Han, A.; Li, L.; Qing, K.; Qi, X.; Hou, L.; Luo, X.; Shi, S.; Ye, F. *Bioorg. Med. Chem.* **2013,** 23, 1310-1314.
9. Molina, P.; Tarraga, A.; Oton, F. *Org. Biomol. Chem.* **2012,** 10, 1711-1724.
10. Townsend, L. B. *Curr. Med. Chem.* **2006,** 13, 1-23.
11. Bahnous, M.; Bouraiou, A.; Chelghoum, M.; Bouacida, S.; Roisnel, T.; Smati, F.; Bentchouala, C.; Gros, P. C.; Belfaitah, A. *Bioorg. Med. Chem. Lett.* **2013,** 23, 1274-1278.
12. Bando, T.; Sugiyama, H. *Acc. Chem. Res*. **2006,** 39, 935-944.
13. Kumar, D.; Thomas, K. R. Justin; Chen, Y. L.; Jou, Y. C.; Jou, J. H. *Tetrahedron* **2013,** 69, 2594-2602.
14. Yuea, S.; Li, N.; Biana, J.; Houb, T.; Mab, J. *Synth. Met.* **2012,** 162, 247-256.
15. Sheludyakov, V. D.; Kuzmina, N. E.; Abramkin, A. M.; Korlyukov, A. A.; Arkhipov, D. E.; Loginov, S. V.; Cheshkov, D. A.; Storozhenko, P. A. *Russ. J. Gen. Chem.* **2011,** 81, 2468-2477.
16. Voronkov, M. G.; Fundamenskii, V. S.; Zelbst, E. A.; Katkevich, Y. V.; Trofimova, O. M.; Bolgova, Y. I.; Chernov, N. F. *Dokl. Chem.* **2005,** 401, 39-41.
17. Singh, G.; Saroa, A.; Garg, M.; Sharma, R. P.; Gubanov, A.I.; Smolentsev, A. I. *J. Organomet. Chem.* **2012,** 719, 21-25.
18. Miao, J.; Wan, H.; Shao, Y.; Guan, G.; Xu, B. *J. Mol. Catal. A: Chem.* **2011,** 348, 77-82.
19. Zhang, Q.; Luo, J.; Wei, Y. *Green Chem.* **2010,** 12, 2246-2254.
20. Yamamoto, T.; Terada, A.; Muramatsu, T.; Ikeda, K. *Org. Prep. Proced. Int.* **1994,** 26, 555-556.
21. Yamamoto, T.; Sugiyama, S.; Akimoto, K.; Hayashi, K. *Org. Prep. Proced. Int.* **1992,** 24, 346-348.
22. Pestunovich, V. A.; Kirpichenko, S. V.; Voronkov, M. G. Silatranes and their tricyclic analogues. In: Z. Rappoport, Y. Apeloig (Eds.), *Chemistry of Organic Silicon Compounds*; Wiley: Chichester, UK, **1998**, 1447-1537.
23. Fujiwara, S. T.; Gushikem Y. *J. Braz. Chem. Soc.*, **1999,** 10, 389-393.

24. Vickers M. S.; Martindale K. S.; Beer, P. D. *J. Mater. Chem.*, **2005,** 15, 2784-2790.
25. Andres, L. S.; Fulscher, M. P.; Roos, B. O. *J. Phys. Chem.* **1996,** 100, 6484-649.
26. Voronkov, M. G.; Trofimova, O. M.; Turchaninov, V. K.; Zelbst, E. A.; Bolgova, Y. I.; Belyaeva, V. V.; Larina L. I.; Aksamentova, T. N.; Mikhaleva A. I.; Chernov N. F. *Russ. J. Org. Chem.*, **2003,** 39, 1458-1466.
27. Garant, R. J.; Daniels, L. M.; Das, S. K.; Janakiraman, M. N.; Jacobson, R. A.; Verkade, J. G. *J. Am. Chem. Soc*. **1991,** 113, 5728-5735.
28. Voronkov, M. G.; Zelbst, E. A.; Kashaev, A. A.; Trofimova, O. M.; Bolgova, Y. I.; Fundamenski, V. S.; Chernov, N. F. *Dokl. Akad. Nauk SSSR* **2001,** 376, 5-7.
29. Carre, F.; Cerveau, G.; Chuit, C.; Corriu, R. J. P.; Nayyar, N. K.; Reye, C. *Organometallics* **1990,** 9, 1989-1991.
30. Stachel, S. J.; Ziller, J. W.; Van Vranken D. L. *Tetrahedron Lett.* **1999,** 40, 5811-5812.
31. Singh, R.; Puri, J. K.; Chahal, V. K.; Sharma, R. P.; Venugopalan, P. *J. Organomet. Chem.* **2010,** 695, 183-188.
32. Dumitriu, A. M. C.; Cazacu, M.; Shova, S.; Turta, C.; Simionescu, B. C. *Polyhedron* **2012,** 33, 119-126.
33. Hencsei, P.; Kovaks, I. *J. Organomet. Chem.* **1989,** 377, 19-23.
34. Hencsei, P.; Pktiyi, L.; Fulop, V.; Baryshok, V. P.; Voronkov M. G., Kuznetsova, G. A. *J. Organomet. Chem.* **1988,** 346, 315-320.
35. Becke, A. D. *J. Chem. Phys.* **1993,** 98, 5648-5652.
36. Lee, C.; Yang, W.; Parr, R. G. *Phys. Rev. B* **1988,** 37, 785-789.
37. Belyaeva, V. V.; Frolov, Y. L.; Voronkov, M. G. *J. Struct. Chem.* **2005,** 46, 1072-1076.
38. Trofimov, A. B.; Zakrzewski, V. G.; Dolgounitcheva, O.; Ortiz, J. V.; Sidorkin, V. F.; Belogolova, E. F.; Belogolov, M.; Pestunovich, V. A. *J. Am. Chem. Soc.* **2005,** 127, 986-995.
39. Shishkov, I. F.; Khristenko, L. V.; Rudakov, F. M.; Golubinskii, A. B.; Vilkov, L. V. Karlov, S. S.; Zaitseva, G. S.; Samdal, S. *Struct. Chem.* **2004,** 15, 11-16.
40. Korlyukov, A. A.; Lyssenko, K. A.; Antipin, M. Y.; Kirin, V. N.; E. A. Chernyshev, E. A.; Knyazev, S. P. *Inorg. Chem.* **2002,** 41, 5043-5051.
41. Alkorta, I.; Elguero, J.; Fruchier, A.; Macquarrie, D. J.; Virgili, A. *J. Organomet. Chem.* **2001,** 625, 148-153.
42. Sharmroukh, A. H.; Zaki, M. E. A.; Morsy, E. M. H.; Abdel-Megeid, F. M. E. *Arch. Pharm.* **2007,** 340, 345-351.
43. Sheldrick, G. M. *SHELXS-97, Program for Structure Solution*, University of Göttingen, **1997**.
44. Sheldrick, G. M. *SHELXL-97, Program for Structure Refinement*, University of Göttingen, **1997**.